2013

Constraining the luminosity function parameters and population size of radio pulsars in globular clusters

Jayanth Chennamangalam

D. R. Lorimer

Ilya Mandel

Manjari Bagchi

Printed 1 July 2018 (MN LATEX style file v2.2)

Constraining the luminosity function parameters and population size of radio pulsars in globular clusters

Jayanth Chennamangalam[1⋆], D. R. Lorimer[1,2], Ilya Mandel[3] and Manjari Bagchi[1]

[1] *Department of Physics, West Virginia University, PO Box 6315, Morgantown, WV 26506, USA*
[2] *NRAO, Green Bank Observatory, PO Box 2, Green Bank, WV 24944, USA*
[3] *School of Physics and Astronomy, University of Birmingham, Edgbaston, Birmingham B15 2TT, UK*

ABSTRACT

Studies of the Galactic population of radio pulsars have shown that their luminosity distribution appears to be log-normal in form. We investigate some of the consequences that occur when one applies this functional form to populations of pulsars in globular clusters. We use Bayesian methods to explore constraints on the mean and standard deviation of the luminosity function, as well as the total number of pulsars, given an observed sample of pulsars down to some limiting flux density, accounting for measurements of flux densities of individual pulsars as well as diffuse emission from the direction of the cluster. We apply our analysis to Terzan 5, 47 Tucanae and M 28, and demonstrate, under reasonable assumptions, that the number of potentially observable pulsars should be within 95% credible intervals of 147^{+112}_{-65}, 83^{+54}_{-35} and 100^{+91}_{-52}, respectively. Beaming considerations would increase the true population size by approximately a factor of two. Using non-informative priors, however, the constraints are not tight due to the paucity and quality of flux density measurements. Future cluster pulsar discoveries and improved flux density measurements would allow this method to be used to more accurately constrain the luminosity function, and to compare the luminosity function between different clusters.

Key words: methods: numerical — methods: statistical — globular clusters: general — globular clusters: individual: Terzan 5, 47 Tucanae, M 28 — stars: neutron — pulsars: general

1 INTRODUCTION

Globular clusters are spherical collections of stars located throughout the haloes of galaxies. Once thought to be composed entirely of old metal-poor population II stars, they are now also believed to form during interactions or collisions of galaxies, therefore containing younger stars having higher metallicities (see Zepf 2003). The total masses of globular clusters range up to the order of $10^6 M_\odot$ (see Meylan & Heggie 1997), and core stellar number densities reach 10^6 pc^{-3}. The high core densities lead to dynamical interactions between stellar systems that are found less commonly in the Galactic plane. For example, globular clusters favour the formation of low-mass X-ray binaries (LMXBs) that are believed to be the progenitors of millisecond pulsars (MSPs; Alpar et al. 1982; Archibald et al. 2009), and hence, the fraction of MSPs among all pulsars in globular clusters is much larger than that in the Galactic field (∼97% versus ∼11%). In addition, the binary MSPs in globular clusters tend to have higher eccentricities compared to their field counterparts, due to exchange or fly-by encounters. MSPs, due to their formation history, can be considered long-lived tracers of LMXBs, and therefore, constraints on the MSP content of globular clusters provide unique insights into binary evolution and the integrated dynamical history of globular clusters, while determining the radio luminosity function of these pulsars helps shed light on the radio emission mechanism in action in these compact objects.

Pulsar searches of globular clusters have yielded impressive returns in recent years (see Camilo & Rasio 2005), with currently 144 pulsars known in 28 clusters[1]. Of these, three clusters, Terzan 5, 47 Tucanae and M 28 are known to harbour more than 10 pulsars each, the most populous being Terzan 5 with 34 (Ransom S. M., private communication). In this paper, we describe a Bayesian method

⋆ E-Mail: jchennam@mix.wvu.edu

[1] See Paulo Freire's globular cluster pulsar catalogue at http://www.naic.edu/∼pfreire/GCpsr.html

that we have developed to compute an estimate of the true number of pulsars in a given cluster, given an observed population. There have been many attempts to constrain the population size of pulsars in all globular clusters in the Galaxy (see, for example, Kulkarni, Narayan & Romani 1990; Bagchi, Lorimer & Chennamangalam 2011). This work is different in that it treats clusters individually instead of dealing with the total population. Bayesian approaches to constrain the pulsar population of individual globular clusters have been used specifically for the case of young (non-recycled) pulsars by Boyles et al. (2011). This work focuses on the entire radio pulsar content of the cluster – the majority of which is made up of old (recycled) pulsars – and additionally, attempts to constrain luminosity function parameters jointly with population size.

Faucher-Giguère & Kaspi (2006) have shown that the luminosity distribution of non-recycled pulsars in the Galactic field appears to be log-normal in form. More recently, Bagchi et al. (2011) have verified that the observed luminosities of recycled pulsars in globular clusters are consistent with this result. Assuming, therefore, that there is no significant difference between the nature of Galactic and cluster populations, we investigate some of the consequences that occur when one applies this functional form to populations of pulsars in individual globular clusters.

For a log-normal (base-10) distribution of pulsar luminosities, the luminosity function is given by

$$f(\log L) = \frac{1}{\sigma\sqrt{2\pi}} e^{-\frac{(\log L - \mu)^2}{2\sigma^2}}, \tag{1}$$

where L is the luminosity in mJy kpc^2, μ is the mean and σ is the standard deviation of the distribution. We are interested in the situation where we observe n pulsars with luminosities above some limiting luminosity $L_{\rm min}$. Given this sample of pulsars, we ask what constraints we can place on their luminosity function parameters, in addition to the potentially observable population size N (that is, the population of pulsars beaming towards the Earth). Another way of thinking about this problem is that there is a family of luminosity function parameters and population sizes that is consistent with an observation of n pulsars above the luminosity limit of the survey, and we are analyzing the posterior probabilities of different members of this family given the observations.

This paper is organized as follows: In §2, we describe our technique. In §3, we apply the technique to observations of a few globular clusters to determine the constraints on the luminosity function parameters and population size. Later, we refine our results using *a priori* information on the luminosity function parameters to get a better estimate of the number of pulsars in those clusters. A summary and our conclusions are presented in §5.

2 BAYESIAN PARAMETER ESTIMATION

Bayes' theorem (see Wall & Jenkins 2003; Gregory 2005), for the purpose of parameter estimation, can be stated mathematically as

$$p(\boldsymbol{\theta}|D, M) = \frac{p(D|\boldsymbol{\theta}, M)p(\boldsymbol{\theta}|M)}{p(D|M)}, \tag{2}$$

where $\boldsymbol{\theta}$ is a set of parameters, D is some data and M is a model describing the parameters. In this notation, $p(\boldsymbol{\theta}|D, M)$ represents the probability of obtaining a set of parameter values given the data and the model, and is termed the *joint posterior probability density*. Similarly, $p(D|\boldsymbol{\theta}, M)$ is the probability of having obtained the observed data, given the parameter values and the model, and is termed the *likelihood*, and $p(\boldsymbol{\theta}|M)$, the *a priori* probability dictated by the model, is termed the *prior probability density*. The denominator, $p(D|M)$ is called the *evidence*, and is just a normalizing factor that can be dropped since we are only interested in relative probabilities, thereby giving

$$p(\boldsymbol{\theta}|D, M) \propto p(D|\boldsymbol{\theta}, M)p(\boldsymbol{\theta}|M). \tag{3}$$

In this paper, we use Bayes' theorem to find the joint posterior probability density functions of the model parameters μ, σ and N given some data. In our case, the data are the individual pulsar flux densities that we call $\{S_i\}$, the observed number of pulsars, n, and the total diffuse flux density of the cluster, $S_{\rm obs}$.

Luminosity is a property intrinsic to pulsars, while flux density is the corresponding observable. The relationship between the two quantities is given by

$$L = \frac{4\pi r^2}{\delta} \sin^2\left(\frac{\rho}{2}\right) \int_{\nu_1}^{\nu_2} S_{\rm mean}(\nu)\, d\nu, \tag{4}$$

where r is the distance to the pulsar, δ is the pulse duty cycle, ρ is the radius of the pulsar emission cone, $S_{\rm mean}(\nu)$ is the mean flux density of the pulsar as a function of observing frequency and ν_1 and ν_2 are the bounds of the frequency range over which the pulsar is observed (see Lorimer & Kramer 2005). Due to the uncertainty associated with the beam geometry, the values of δ and ρ are not generally reliable for luminosity calculations. Therefore, we use a simplified model of the luminosity, the 'pseudo-luminosity', that is defined as $L_\nu = S_\nu\ r^2$ at a given frequency ν (the subscript ν on L and S will be dropped for the rest of the paper). As can be inferred from Equation (4) and the aforementioned pseudo-luminosity equation, the luminosity function is inevitably corrupted by uncertainties in distance. To mitigate this, we decided to perform our analysis initially in terms of the measured flux densities, and later, use a model of distance uncertainty to convert our results to the luminosity domain. We take the distance to all pulsars in a globular cluster to be the same. The log-normal in luminosity can then alternatively be written in terms of the flux density. The probability of detecting a pulsar with flux density S in the range $\log S$ to $\log S + d(\log S)$ is then given by a log-normal in S as

$$p(\log S)\ d(\log S) = \frac{1}{\sigma_S\sqrt{2\pi}} e^{-\frac{(\log S - \mu_S)^2}{2\sigma_S^2}}\ d(\log S), \tag{5}$$

where S is in mJy, and μ_S and σ_S are the mean and standard deviation of the *flux density distribution*. The probability of observing a pulsar above the limit $S_{\rm min}$ is then

$$\begin{aligned} p_{\rm obs} &= \int_{\log S_{\rm min}}^{\infty} p(\log S)\ d(\log S) \\ &= \frac{1}{2}\ {\rm erfc}\left(\frac{\log S_{\rm min} - \mu_S}{\sqrt{2}\sigma_S}\right). \end{aligned} \tag{6}$$

Our analysis involves computing three likelihoods in the

flux domain based on three sets of data, computing the total likelihood as the product of these three likelihoods, converting this flux domain likelihood to the luminosity domain, and subsequently, applying priors to obtain the posterior. This procedure is depicted graphically in the block diagram of Figure 1.

2.1 Using pulsar flux densities

In the first step, we consider as data the measured flux densities of the pulsars in the cluster under scrutiny, that we call $\{S_i\}$. Ideally, the survey sensitivity limit $S_{\rm min}$ can be taken as another datum, but its exact value is not always known. The effects of radiometer noise, Doppler smearing, interference, and in some cases, interstellar scintillation, result in a distribution of $S_{\rm min}$. We decided, therefore, to parametrize $S_{\rm min}$. The likelihood of observing a set of pulsars with fluxes $\{S_i\}$ is represented as

$$\prod_{i=1}^{n} p_i(\log S_i|\mu_S, \sigma_S, S_{\rm min}),$$

where n is the number of observed pulsars in the cluster. Each term in this product is given by

$$p_i(\log S_i|\mu_S, \sigma_S, S_{\rm min}) = \frac{1}{p_{\rm obs}\sigma_S\sqrt{2\pi}} e^{-\frac{(\log S_i - \mu_S)^2}{2\sigma_S^2}}, \quad (7)$$

where $p_{\rm obs}$ is as given in Equation (6). This likelihood is represented as 'Likelihood A' in Figure 1. Uncertainties in the flux density measurements are not considered here, but note that ignoring them will have the effect of underestimating the width of posterior credible intervals. In §4.1, we discuss the effects of ignoring the errors associated with flux density measurements.

2.2 Incorporating the number of observed pulsars

To infer the total number of pulsars N in the cluster, we follow Boyles et al. (2011) to take as likelihood the probability of observing n pulsars in a cluster with N pulsars, given by the binomial distribution

$$p(n|N, \mu_S, \sigma_S, S_{\rm min}) = \frac{N!}{n!(N-n)!}\, p_{\rm obs}^{n}\, (1-p_{\rm obs})^{N-n}, \quad (8)$$

where $p_{\rm obs}$ is computed as in Equation (6). This likelihood is shown as 'Likelihood B' in Figure 1.

2.3 Considering diffuse emission

Next, we incorporate information about the observed diffuse flux $S_{\rm obs}$ from the direction of the globular cluster. We assume that all radio emission is due to the pulsars in the cluster, including both detected pulsars and the unresolved background. Unlike standard pulsar searches, imaging the diffuse radio emission of a cluster to estimate the number of pulsars therein, is not affected by phenomena that cause pulse broadening, such as dispersion or scattering, or the fact that some of the pulsars in the cluster are in accelerating frames (Fruchter & Goss 1990). For the likelihood of measuring the diffuse flux $S_{\rm obs}$, we choose

$$p(S_{\rm obs}|N, \mu_S, \sigma_S) = \frac{1}{\sigma_{\rm diff}\sqrt{2\pi}}\, e^{-\frac{(S_{\rm obs} - S_{\rm diff})^2}{2\sigma_{\rm diff}^2}}, \quad (9)$$

where $S_{\rm diff}$ is the expectation of the total diffuse flux of a cluster whose flux density distribution is a log-normal with parameters μ_S and σ_S, and having N pulsars, and $\sigma_{\rm diff}$ is the standard deviation of this distribution. This likelihood is referred to as 'Likelihood C' in Figure 1. Assuming that the cluster contains N pulsars, each having average luminosity,

$$S_{\rm diff} = N\langle S\rangle, \quad (10)$$

and

$$\sigma_{\rm diff} = \sqrt{N}\ {\rm SD}(S), \quad (11)$$

where the expectation of S,

$$\langle S\rangle = 10^{\mu_S + \frac{1}{2}\sigma_S^2 \ln(10)}, \quad (12)$$

and the standard deviation of S,

$$ {\rm SD}(S) = 10^{\mu_S + \frac{1}{2}\sigma_S^2 \ln(10)} \sqrt{10^{\sigma_S^2 \ln(10)} - 1}. \quad (13)$$

We do not consider the uncertainty in the diffuse flux measurement, and as mentioned in §2.1, this has the effect of underestimating the credible intervals on our posteriors.

The total likelihood, then,

$$\begin{aligned} &p(\log S_i, n, S_{\rm obs}|N, \mu_S, \sigma_S, S_{\rm min}) \\ &\quad = \prod_{i=1}^{n} p_i(\log S_i|\mu_S, \sigma_S, S_{\rm min}) \\ &\qquad \times p(n|N, \mu_S, \sigma_S, S_{\rm min}) \\ &\qquad \times p(S_{\rm obs}|N, \mu_S, \sigma_S). \end{aligned} \quad (14)$$

2.4 Transformation to luminosity domain

The flux density distribution of pulsars in a globular cluster, although proportional to their luminosity distribution, is not suitable for comparing the populations in different clusters, as it depends on the distance to the cluster. It is, therefore, useful to transform the total likelihood obtained in the previous subsection to the luminosity domain. We convert the total likelihood of Equation (14) to the luminosity domain in the following way. Since the pseudo-luminosity equation can be written in terms of logarithms as $\log L = \log S + 2\log r$, where L is in mJy kpc^2, S is in mJy, and r is in kpc, the means of the two distributions are related additively by the term $2\log r$, while the standard deviations are the same. Taking into account the uncertainty in distance, we have a distribution of distances, $p(r)$. The total likelihood in the luminosity domain is

$$\begin{aligned} &p(\log S_i, n, S_{\rm obs}|N, \mu, \sigma, S_{\rm min}, r) \\ &\qquad = p(\log S_i, n, S_{\rm obs}|N, \mu_S, \sigma_S, S_{\rm min}), \end{aligned} \quad (15)$$

where μ and μ_S are related additively as mentioned above, and σ and σ_S are equal. The final joint posterior in luminosity is then given by

$$\begin{aligned} &p(N, \mu, \sigma, S_{\rm min}, r|\log S_i, n, S_{\rm obs}) \\ &\quad \propto\ p(\log S_i, n, S_{\rm obs}|N, \mu, \sigma, S_{\rm min}, r) \\ &\qquad \times p(N)\ p(\mu)\ p(\sigma)\ p(S_{\rm min})\ p(r). \end{aligned} \quad (16)$$

The prior on N is taken to be uniform from n to ∞, where the upper limit, for the sake of computation, would be a sufficiently large value. We also use uniform priors on the model parameters μ and σ. Due to the nature of the uncertainty in determining the exact value of $S_{\rm min}$, we choose

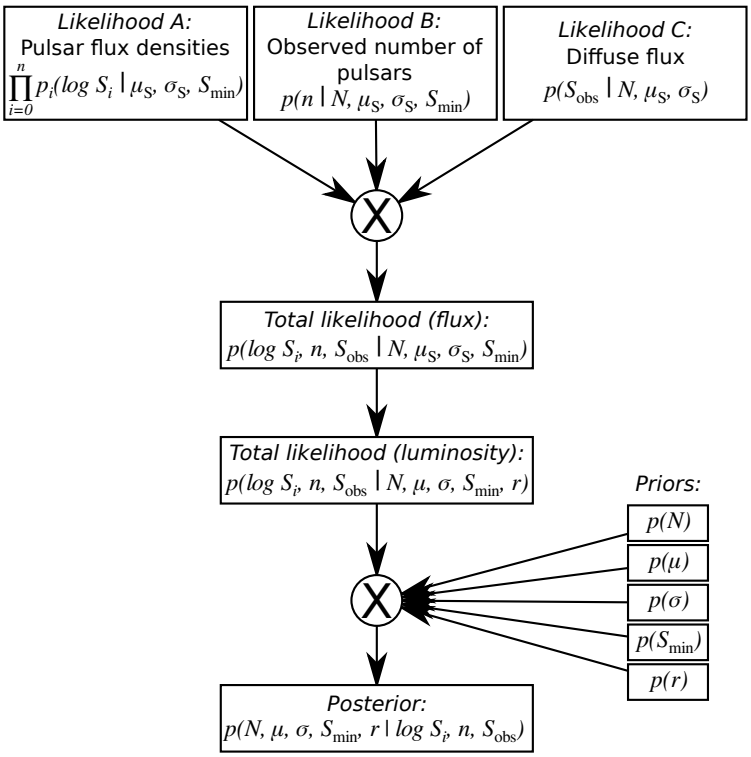

Figure 1. Logical flow of the Bayesian analysis. The circle with the × sign symbolizes a multiplication operation.

a uniform prior on it in the range (0, min(S_i)], where the upper limit is the flux density of the least bright pulsar in the cluster. The prior on r is taken to be a Gaussian. This joint posterior is then integrated over various sets of model parameters to obtain marginalized posteriors.

3 APPLICATIONS

We applied our Bayesian technique[2] to the globular clusters Terzan 5, 47 Tucanae and M 28 (although the clusters we consider contain only recycled known pulsars, the analysis would remain the same even if there were young pulsars in the sample). The choice of clusters was based on the amount of data available. Terzan 5 is the cluster most-suited for this analysis due to the fact that it has a relatively large number of pulsars for which flux density measurements are available. Although Terzan 5 has 34 known pulsars (Ransom S. M., private communication), we take $n = 25$, the number of pulsars for which we have flux density measurements. The flux densities of the individual pulsars were collected in a literature survey (Bagchi et al. 2011, and references therein), with the values relevant to this work reproduced in Table 1. For Terzan 5, the flux densities we used were scaled from those reported at 1950 MHz by Ransom et al. (2005) and Hessels et al. (2006) to 1400 MHz using a spectral index, $\alpha = -1.9$ (the mean value for globular cluster MSPs), using the power law $S(\nu) \propto \nu^{\alpha}$. Hessels et al. (2007) and Bagchi et al. (2011) discuss the choice of spectral index in detail. The observed diffuse flux density at 1400 MHz is taken to be $S_{obs} = 5.2$ mJy (the sum of the diffuse flux and the fluxes of point sources as reported by Fruchter & Goss 2000). The priors used were formed in the following ways. The prior on N was chosen to be a uniform distribution in the range [n, 500], where the upper limit is 150% of the upper limit obtained by Bagchi et al. (2011) (using the values of μ and σ as found by Faucher-Giguère & Kaspi 2006) above their upper limit. We note that this prior is sufficiently wide to ensure that the posterior does not rail against the prior boundaries. We chose uniform distributions in the same range of μ and σ as used by Bagchi et al. (2011) as our priors, namely, [-2.0, 0.5] and [0.2, 1.4], respectively. Survey sensitivity limits were not always available, and additionally, due to a variety of factors mentioned in §2.1, for all of our analyses, we took S_{min} to be a uniform distribution in the range (0, min(S_i)]. The most recent measurement of the distance to Terzan 5, $r = 5.5 \pm 0.9$ kpc (Ortolani et al. 2007), was used to model the distance prior. We modelled the distance prior as a Gaussian with mean 5.5 kpc and standard deviation 0.9 kpc. Figure 2 shows the results of the analysis for Terzan 5. The mode of the marginalized posterior on N, shown in Figure 2(b), is 43 and the median with the surrounding 95% credible interval is 142^{+310}_{-110}. As can be seen from Figures 2(b), 2(c) and 2(d), the constraints we obtain on N, μ and σ, respectively, are broad, due to a dearth of flux density measurements. The marginalized posterior on S_{min}, plotted in Figure 2(e), shows a strong preference for values away from 0 and closer to that of the least bright pulsar observed. The main results are tabulated in Table 2.

For 47 Tucanae and M 28, containing 14 and 9 pulsars each, the individual flux densities used are given in Table 1.

[2] The software package that we developed to perform the analysis described in this paper is available freely for download from http://psrpop.phys.wvu.edu/gcbayes/.

We took $S_{\rm obs} = 2.0$ mJy (1400 MHz flux as reported by McConnell et al. 2004) for 47 Tucanae, and $S_{\rm obs} = 1.8$ mJy (1400 MHz flux as reported by Kulkarni et al. 1990) for M 28. The priors on N were taken to be uniform in the intervals $[n,\ 225]$ for 47 Tucanae and $[n,\ 400]$ for M 28, where the upper limits were computed in the same way as we did for Terzan 5. Priors on $S_{\rm min}$ were formed as in the case of Terzan 5, in the range $(0,\ \min(S_i)]$. The latest distance measurement of 4.69 ± 0.17 kpc (Woodley et al. 2012) was used to form the distance prior for 47 Tucanae. For M 28, we used $r = 5.5 \pm 0.3$ kpc (Servillat et al. 2012). The main results for these clusters are tabulated in Table 2.

The value of N can be further refined by considering possible dependences on other physical parameters of globular clusters. In a forthcoming paper (Turk & Lorimer 2013, in prep.), an empirical Bayesian approach is being applied to the set of 95 flux density limits for globular clusters presented in Boyles et al. (2011) in which pulsar abundance as a function of two-body encounter rate, metallicity, cluster mass, etc. is incorporated into the likelihood functions. Note that N is the size of the population of pulsars in the cluster that are beaming towards the Earth. We can include the beaming fraction – the fraction of all pulsars beaming towards us – to refine this estimate. Uncertainties notwithstanding, the beaming fraction of millisecond pulsars is generally thought to be greater than 50% (Kramer et al. 1998). This, together with the fact that most pulsars in globular clusters are millisecond pulsars, imply that the true population size in a cluster is approximately a factor of two more than the potentially observable population size.

3.1 Using prior information

In the framework developed in the previous section, we use broad uniform (non-informative) priors for the mean and standard deviation of the log-normal. This lack of prior information is apparent in Figure 2(b), where N is not very well constrained. Prior information can help better constrain the parameters of interest. Boyles et al. (2011) use models of non-recycled Galactic pulsars from Ridley & Lorimer (2010) to narrow down μ to between -1.19 and -1.04, and σ to the range 0.91 to 0.98. We assume that these values are applicable to the globular cluster pulsars based on Bagchi et al. (2011) who draw the conclusion that the luminosity function of cluster pulsars is no different from that of the Galactic disc as found by Faucher-Giguère & Kaspi (2006). The values themselves are also consistent with the results of Bagchi et al. (2011). We choose μ and σ to be uniform within these ranges. Applying the Bayesian analysis over this narrower range of μ and σ for Terzan 5 results in much tighter constraints on N as seen in Figure 3(a), in which the mode of the distribution is 136 and the median and a 95% credible interval is 147^{+112}_{-65}. The analysis was also performed for 47 Tucanae and M 28, the results of which are given in Figures 3(b) and 3(c), respectively. For 47 Tucanae, the mode of N is 79 and the median with the surrounding 95% credible interval is 83^{+54}_{-35}. For M 28, the mode is 91 and the median with credible interval is 100^{+91}_{-52}. Our result for Terzan 5 is consistent with that of Bagchi et al. (2011). In the case of 47 Tucanae and M 28, there is partial, yet considerable overlap between our credible ranges and the corresponding confidence intervals of

Table 1. Flux densities used in the analysis.

Pulsar	1400 MHz Flux Density (mJy)
Terzan 5	
J1748−2446A	1.91[a]
J1748−2446C	0.68[a]
J1748−2446D	0.08[a]
J1748−2446E	0.09[a]
J1748−2446F	0.07[a]
J1748−2446G	0.03[a]
J1748−2446H	0.03[a]
J1748−2446I	0.05[a]
J1748−2446J	0.04[a]
J1748−2446K	0.08[a]
J1748−2446L	0.08[a]
J1748−2446M	0.06[a]
J1748−2446N	0.10[a]
J1748−2446O	0.23[a]
J1748−2446P	0.14[a]
J1748−2446Q	0.05[a]
J1748−2446R	0.02[a]
J1748−2446S	0.03[a]
J1748−2446T	0.04[a]
J1748−2446U	0.03[a]
J1748−2446V	0.13[a]
J1748−2446W	0.04[a]
J1748−2446X	0.03[a]
J1748−2446Y	0.03[a]
J1748−2446ad	0.15[b]
47 Tucanae	
J0023−7204C	0.36[c]
J0024−7204D	0.22[c]
J0024−7205E	0.21[c]
J0024−7204F	0.15[c]
J0024−7204G	0.05[c]
J0024−7204H	0.09[c]
J0024−7204I	0.09[c]
J0023−7203J	0.54[c]
J0024−7204L	0.04[c]
J0023−7205M	0.07[c]
J0024−7204N	0.03[c]
J0024−7204O	0.10[c]
J0024−7204Q	0.05[c]
J0024−7203U	0.06[c]
M 28	
B1821−24A	0.94[d]
J1824−2452B	0.07[d]
J1824−2452C	0.17[d]
J1824−2452D	0.05[d]
J1824−2452E	0.06[d]
J1824−2452F	0.08[d]
J1824−2452G	0.05[d]
J1824−2452H	0.06[d]
J1824−2452J	0.07[d]

[a] Based on values reported by Ransom et al. (2005). The fractional uncertainties on these values are $\sim 30\%$.
[b] Based on the value reported by Hessels et al. (2006). The fractional uncertainty on this value is 25%.
[c] Camilo et al. (2000). The fractional uncertainties on these values range from 10% to 40%.
[d] Bégin (2006). The reported values are 'highly uncertain'.

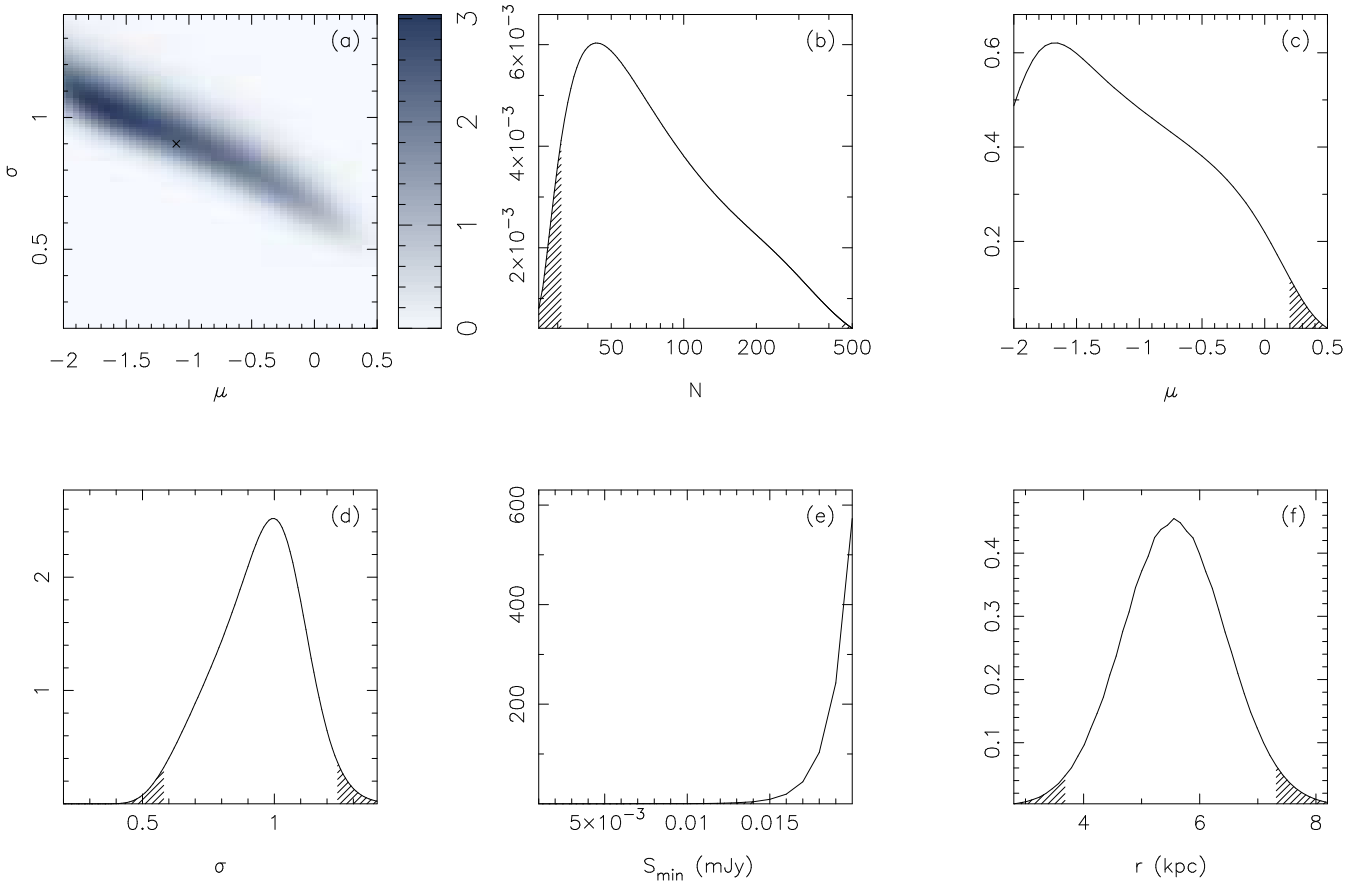

Figure 2. Results of the Bayesian analysis for Terzan 5, with $\{S_i\}$ as given in Table 1, $n = 25$, and $S_{\rm obs} = 5.2$ mJy. This analysis was run with wide priors on μ and σ, with the ranges equal to those used by Bagchi et al. (2011) (their Figure 2). (a) depicts the joint posterior on μ and σ, marginalized over N, $S_{\rm min}$ and r. The '×' symbol marks the intersection of the values obtained by Faucher-Giguère & Kaspi (2006); (b) is the marginalized posterior for N, with a mode of 43 and a median of 142. The x-axis is plotted in log scale for clarity; (c) is the marginalized posterior for μ with a mode of -1.65 and a median of -1.2; (d) is the marginalized posterior for σ with a mode of 1.0 and a median of 0.95; (e) is the marginalized posterior for $S_{\rm min}$ with both mode and median equal to 0.02 mJy; (f) is the marginalized posterior for r, with both mode and median equal to 5.56 kpc. The hatching indicates regions that lie outside a 95% credible interval.

Bagchi et al. (2011). For 47 Tucanae, our results agree with those of Grindlay et al. (2002), i.e., 35–90 MSPs with X-ray luminosities above 10^{30} erg s^{-1}. However, our result for 47 Tucanae is inconsistent with that of McConnell et al. (2004) who estimate $N \leqslant 30$. This disparity may be due to the high scintillation of the pulsars in this cluster affecting both individual as well as diffuse flux measurements. The results of our analyses are tabulated in Table 2.

4 DISCUSSION

4.1 Effect of flux density measurement errors on credible intervals

Our analysis in its present form does not take into account measurement uncertainties of pulsar flux densities. This leads to an underestimation of our credible intervals and in this section, we discuss the effect that neglecting measurement errors has on our credible intervals. We performed a Monte Carlo simulation in which the flux density corresponding to each Terzan 5 pulsar was modelled as a Gaussian with mean equal to the measured value (given in Table 1) and standard deviation equal to the measurement

Table 2. Median and 95% credible intervals from the various analyses presented in this paper. We note here that, in addition to the sources of error mentioned in the text, the values of μ and σ presented here are also affected by the fact that computations are discrete and hence use a finite number of steps. Note that for the case of narrow priors on μ and σ, the corresponding two columns do not carry any useful information, reflecting merely the ranges of the priors, and are included here only for completeness.

Cluster	N	μ	σ
Wide priors on μ and σ			
Ter 5	142^{+310}_{-110}	$-1.2^{+1.4}_{-0.8}$	$1.0^{+0.3}_{-0.4}$
47 Tuc	39^{+169}_{-25}	$-0.6^{+0.9}_{-1.3}$	$0.7^{+0.4}_{-0.4}$
M 28	198^{+191}_{-169}	$-1.3^{+1.1}_{-0.7}$	$0.8^{+0.3}_{-0.3}$
Narrow priors on μ and σ			
Ter 5	147^{+112}_{-65}	$-1.12^{+0.08}_{-0.07}$	$0.94^{+0.03}_{-0.03}$
47 Tuc	83^{+54}_{-35}	$-1.13^{+0.08}_{-0.07}$	$0.94^{+0.04}_{-0.03}$
M 28	100^{+91}_{-52}	$-1.13^{+0.09}_{-0.06}$	$0.94^{+0.04}_{-0.03}$

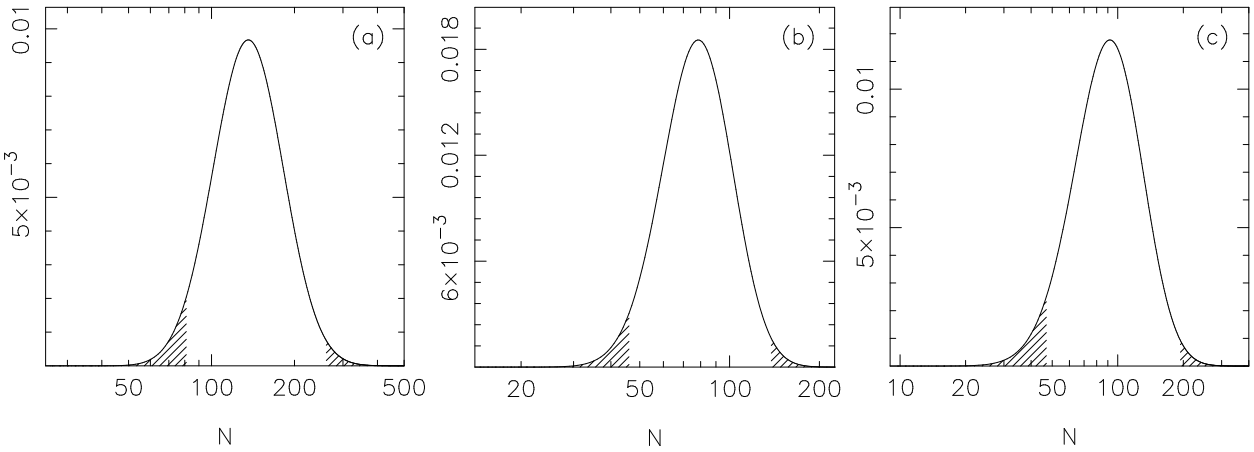

Figure 3. Posteriors on N after applying the Boyles et al. (2011) priors on μ and σ: (a) Terzan 5, with $n = 25$ and $S_{\rm obs} = 5.2$ mJy. The median with the surrounding 95% credible interval of N is 147^{+112}_{-65}; (b) 47 Tucanae, with $n = 14$ and $S_{\rm obs} = 2.0$ mJy. The median with credible interval is 83^{+54}_{-35}; (c) M 28, with $n = 9$ and $S_{\rm obs} = 1.8$ mJy. The median with credible interval is 100^{+91}_{-52}. The flux densities of the individual pulsars, $\{S_i\}$, used in this analysis are given in Table 1.

error (given in the footnotes to Table 1). A flux density value was picked for each pulsar from these distributions and our Bayesian analysis performed on the new set of flux densities. The analysis was done with both wide and narrow priors on μ and σ, resulting in two sets of credible intervals. For non-informative priors, the standard deviation on the lower limit of the credible interval for N was found to be 7 while that on the upper limit was 165. For narrow priors, the standard deviation on the lower limit was 19 while that on the upper limit was 75. This simplified simulation of the impact of unmodelled measurement uncertainties suggests that the lower limits of the 95% credible intervals are fairly robust, while their upper limits may vary by about one half of the values given in Table 2. A more accurate simulation would involve generating sets of flux densities according to all the priors in our analysis, with added dither due to the unmodelled measurement uncertainty, and for each set, compute the 95% credible intervals using our technique, and check what fraction of true values lies outside these intervals. Such a simulation, although more accurate, would be computationally expensive. In principle, measurement uncertainties could be included directly in the likelihood model, and marginalized over to compute the posteriors of interest.

4.2 Effect of increasing detections on credible intervals

In order to gauge the performance of our technique with respect to increasing pulsar detections and subsequent flux density measurements, we performed the following Monte Carlo simulation. We simulated a globular cluster with population size equal to our wide-prior median estimate for Terzan 5, 142 pulsars, located at the distance of Terzan 5, whose luminosity follows a log-normal with μ and σ fixed at the Faucher-Giguère & Kaspi (2006) values of -1.1 and 0.9, respectively. For this cluster, we varied the survey sensitivity limit, and at each step, counted the observed number of pulsars, and ran our Bayesian analysis, giving us a set of credible intervals. The Bayesian analysis was done with the same priors as in the first part of §3, viz. uniform prior on N in the range $[n, 500]$, uniform prior on $S_{\rm min}$ in the range $(0, \min(S_i)]$, and the uniform, wide Bagchi et al. (2011) priors on μ and σ. This process was then repeated for multiple Monte Carlo realizations of the log-normal to allow for flux density variations to be manifested. The results are given in Figure 4 where the width of the credible intervals on the parameters N, μ and σ are plotted against the number of pulsars detected. As expected, there is a clear improvement in the credible interval widths with the number of pulsars. Since our population estimate of 142 indicates that we have already detected about a fifth of the potentially observable pulsars in Terzan 5, increasing the number of detections/flux density measurements by, say, a factor of 2 would improve our credible interval on N by approximately 15%, whereas the credible intervals on μ an σ would improve by about 15% and 10%, respectively.

5 SUMMARY AND CONCLUSIONS

We have developed a Bayesian technique to constrain the luminosity function parameters and population size of pulsars in individual globular clusters, given a data set that consists of the number of observed pulsars, the flux densities of the individual pulsars in the cluster and the total diffuse flux emission from the direction of the globular cluster, assuming a log-normal luminosity function. We have applied our analysis to a few globular clusters and have demonstrated the utility of this technique in constraining the aforementioned parameters.

Our technique is applied in two different ways – first, with no prior information, and second, assuming prior knowledge of the possible ranges of μ and σ. As shown for Terzan 5, the results for the first approach do not constrain N, μ or σ very well due to paucity of data, but the latter two do exhibit consistency with the values found by Faucher-Giguère & Kaspi (2006) and Bagchi et al. (2011). For the second approach in which we assume prior informa-

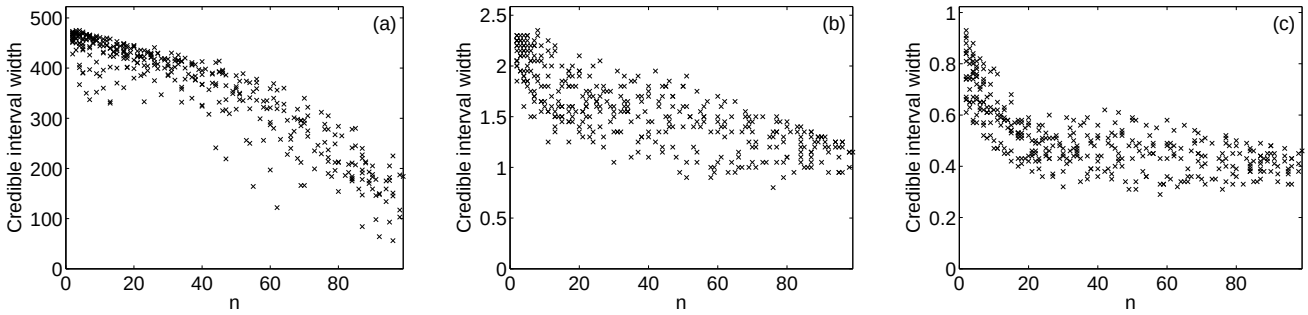

Figure 4. Results of the Monte Carlo simulation described in §4.2. (a) shows how the width of the credible interval on N decreases with increasing number of detected pulsars, n. (b) and (c) correspond to credible intervals on μ and σ, respectively.

tion to bound μ and σ, the priors help better constrain the total number of pulsars in the cluster.

The technique we have developed here should prove useful in future studies of the globular cluster luminosity function where ongoing and future pulsar surveys are expected to provide a substantial increase in the observed populations of pulsars in many clusters. In particular, we anticipate that the increased amount of data would enable us to constrain the distributions of μ and σ independently (i.e. without the need to assume prior information from the Galactic pulsar population). Further interferometric measurements of the diffuse radio flux in many globular clusters could provide improved constraints on μ and σ by measuring the flux contribution from the individually unresolvable population of pulsars.

ACKNOWLEDGMENTS

We thank the anonymous referee for useful comments. We thank Phil Turk and Nipuni Palliyaguru for useful discussions. This work was supported by a Research Challenge Grant to the WVU Center for Astrophysics by the West Virginia EPSCoR foundation, and also by the Astronomy and Astrophysics Division of the National Science Foundation via a grant AST-0907967.

REFERENCES

Alpar M. A., Cheng A. F., Ruderman M. A., Shaham J., 1982, Nat, 300, 728

Archibald A. M., Stairs I. H., Ransom S. M., Kaspi V. M., Kondratiev V. I., Lorimer D. R., McLaughlin M. A, Boyles J., Hessels J. W. T., Lynch R., van Leeuwen J., Roberts M. S. E., Jenet F., Champion D. J., Rosen R., Barlow B. N., Dunlap B. H., Remillard R. A., 2009, Sci, 324, 1411

Bagchi M., Lorimer D. R., Chennamangalam J., 2011, MNRAS, 418, 477

Bégin S., 2006, Ph.D. Thesis, UBC

Boyles J., Lorimer D. R., Turk P. J., Mnatsakanov R., Lynch R. S., Ransom S. M., Freire P. C., Belczynski K., 2011, ApJ, 742, 51

Camilo F., Rasio F. A., 2005, in Rasio F. A., Stairs I. H., eds, ASP Conf. Ser. Vol. 328, Binary Radio Pulsars. Astron. Soc. Pac., San Francisco, p.147

Camilo, F., Lorimer D. R., Freire P., Lyne A. G., Manchester R. N., 2000, ApJ, 535, 975

Faucher-Giguère C.-A., Kaspi V. M., 2006, ApJ, 643, 332

Fruchter A. S., Goss W. M., 1990, ApJ, 365, L63

Fruchter A. S., Goss W. M., 2000, ApJ, 536, 865

Gregory P. C., 2005, Bayesian Logical Data Analysis for the Physical Sciences: A Comparative Approach with *Mathematica* Support. Cambridge University Press, Cambridge, UK

Grindlay J. E., Camilo F., Heinke C. O., Edmonds P. D., Cohn H., Lugger P., 2002, ApJ, 581, 470

Hessels J. W. T., Ransom S. M., Stairs I. H., Kaspi V. M., Freire P. C. C., 2007, ApJ, 670, 363

Hessels J. W. T., Ransom S. M., Stairs I. H., Freire P. C. C., Kaspi V. M., Camilo F., 2006, Sci, 311, 1901

Kulkarni S. R., Goss W. M., Wolszczan A., Middleditch J., 1990, ApJ, 363, L5

Kulkarni S. R., Narayan R., Romani R. W., 1990, ApJ, 356, 174

Kramer M., Xilouris K. M., Lorimer D. R., Doroshenko O., Jessner A., Wielebinski R., Wolszczan A., Camilo F., 1998, ApJ, 501, 270

Lorimer D. R., Kramer M., 2005, Handbook of Pulsar Astronomy, Cambridge Univ. Press, Cambridge, UK

McConnell D., Deshpande A. A., Connors T., Ables J. G., 2004, MNRAS, 348, 1409

Meylan G., Heggie D. C., 1997, A&AR, 8, 1

Ortolani S., Barbuy B., Bica E., Zoccali M., Renzini A., 2007, A&A, 470, 1043

Ransom S. M., Hessels J. W. T., Stairs I. H., Freire P. C. C., Camilo F., Kaspi V. M., Kaplan D. L., 2005, Sci, 307, 892

Ridley J. P., Lorimer D. R., 2010, MNRAS, 404, 1081

Servillat M., Heinke C. O., Ho W. C. G., Grindlay J. E., Hong J., van den Berg M., Bogdanov S., 2012, MNRAS, 423, 1556

Turk P. J., Lorimer D. R., 2013, in prep.

Wall J. V., Jenkins C. R., 2003, Practical Statistics for Astronomers. Cambridge Univ. Press, Cambridge, UK

Woodley K. A., Goldsbury R., Kalirai J. S., Richer H. B., Tremblay P.-E., Anderson J., Bergeron P., Dotter A., Esteves L., Fahlman G. G., Hansen B. M. S., Heyl J., Hurley J., Rich R. M., Shara M. M., Stetson P. B., 2012, AJ, 143,

50
Zepf S. E., 2003, in Engvold O., ed, Highlights of Astronomy, Vol. 13, as presented at the XXVth General Assembly of the IAU 2003, Astron. Soc. Pac., San Francisco, p. 347